

DOI: 10.1002/adma.200701840

Chitosan Nanostructures with Controllable Morphology Produced by a Nonaqueous Electrochemical Approach**

By Jingming Gong, Xianluo Hu, Ka-wai Wong,* Zhi Zheng, Lin Yang, Woon-ming Lau, and Ruxu Du

As we enter the era of bio-nanotechnology, nanomaterials are playing a new and important role in many biology-related applications and advanced nanodevices.^[1] In particular, those conjugated with biological moieties have enormous potential in biolabeling, drug delivery, and therapeutic applications. In fact, much progress has been achieved in the past ten years based on inorganic (e.g., CdSe, Au) nanomaterials.^[2] However, these inorganic compounds raise significant environment concerns and represent potential danger for more extensive medical diagnostics and applications, especially in *in vitro* and *in vivo* tests and applications. In addition, some of them, for example, Cd-based compounds, are well-known toxicants and carcinogens to humans. Furthermore, different surface functionalizations are always required for these inorganic nanomaterials so that they can effectively bind to different biological substances such as DNA, proteins, and viruses. These facts prompt the need for nanomaterials with high biocompatibility and bioaffinity. Naturally, bio-organic substances are perfect candidates, however, successful syntheses of bio-organic nanomaterials are lacking to a high degree, in spite of some outstanding achievements based on peptides.^[3] Those with controllable morphology on a nanometer scale are even rarer, despite the fact that the geometrical size and shape are influential factors for adapting biological substances such as

cells, bacteria, and proteins, whose behavior is very sensitive to the geometric size and shape of the surrounding environment.

Chitosan, a deacetylation product of chitin, is a functional and basic polysaccharide composed of β -1,4-linked glucosamine, which can be easily extracted from the exoskeletons of shrimps and crabs.^[4] Owing to its special properties, for example, nontoxicity, biodegradability, biocompatibility, and antimicrobial activity,^[5,6] this polycationic biopolymer is receiving a great deal of attention for biosensing, medical, and pharmaceutical applications.^[7] Also, it is the most commonly used natural polymer in regenerative medicine and tissue engineering.^[8] Chitosan micro- or nanofibers have been widely accepted as biomedical scaffolding materials to restore, maintain, or improve the functions of various tissues.^[9] Therefore, the creation of chitosan nanostructures with controllable morphology is highly desirable, but has met with limited success yet. Recently, one elegant method, electrospinning, has been reported for producing chitosan nanofibers.^[10] Electrospinning allows fabrication of chitosan nanofibers under high-voltage conditions (15–25 kV). The nanofibers prepared are, however, all amorphous with only thread-like morphology.

In this Communication, we report a facile nonaqueous electrochemical approach to synthesizing different single-crystal chitosan nanostructures on a stainless steel substrate, without using a template, catalyst, or surfactant. It is well known that chitosan is a compound with both strong inter- and intramolecular hydrogen bonding interactions due to the presence of hydroxyl and amino groups. Also, with these functional groups, chitosan has an intrinsically strong affinity to many different types of biological substances without specific modifications. In our approach, we expected that the subtle variations of these hydrogen-bonding interactions under the applied electric field would act as the driving force to direct the anisotropic growth of different chitosan nanostructures. Although the exact growth mechanism still remains not clearly identified, it was solidly demonstrated that the nanoscale morphology of chitosan can be adjusted by tuning the reaction conditions during electrochemical synthesis. Because of their biocompatibility and biodegradability, the resulting chitosan nanostructures can be potentially tailored to mimic a natural extracellular matrix, to achieve controlled drug delivery, and to develop tissue-compatible scaffolds for tissue cultures. To the best of our knowledge, this is the first report on the fabrication of single-crystal chitosan nanostructures by an electrochemical

[*] Prof. K.-W. Wong, Dr. J. M. Gong, Dr. X. L. Hu, Prof. Z. Zheng
Prof. R. X. Du

Institute of Precision Engineering and Department of Physics
The Chinese University of Hong Kong
Shatin, New Territories, Hong Kong SAR (P.R. China)
E-mail: kwong@cuhk.edu.hk

Dr. J. M. Gong
Key Laboratory of Pesticides and Chemical Biology of
Ministry of Education
College of Chemistry
Central China Normal University
Wuhan 430079 (P.R. China)

Prof. L. Yang
College of Chemistry and Environmental Science
Henan Normal University
Xinxiang 453007 (P.R. China)

Prof. W.-M. Lau
Surface Science
Western University of Western Ontario
London, Ontario N6A 5B7 (Canada)

[**] This work was financially supported by the Institute of Precision Engineering and Department of Physics, The Chinese University of Hong Kong. Supporting Information is available online from Wiley InterScience or from the authors.

approach. The synthetic process is simple and can be performed under mild and usual experimental laboratory conditions. It provides a facile and moderate approach to synthesizing single-crystal chitosan nanostructures.

In a typical preparation, as-received chitosan powder was firstly dispersed in propylene carbonate (PC) under mild ultrasonication (70 W). The pH of the chitosan solution was adjusted to ca. 4.5 by adding an appropriate amount of sulfuric acid (H_2SO_4). LiClO_4 (5.5 mM) was used as the supporting electrolyte during the electrochemical process. The general morphology of the product was studied by scanning electron microscopy (SEM). Figures 1a and b show representative SEM images of the chitosan nanowires as deposited at $E = -3$ V versus Ag/AgCl. Evidently, the chitosan nanowires prepared are quite uniform in dimension and size, and straight along the longitudinal axis. The nanowires have an average diameter of ca. 70–80 nm and a length of up to ca. 3 μm . The inset in Figure 1b is a high-magnification SEM image. Interestingly, these nanowires exhibit a rectangular cross section. The detailed microstructure of the chitosan nanowires was further characterized by transmission electron microscopy (TEM). Figure 1c displays a typical TEM image of an individual chitosan nanowire with a diameter of ca. 100 nm and a length of 1.5 μm . Its corresponding electron diffraction (ED) pattern was obtained. As shown in Figure 1d, distinct and sharp spot reflections are clearly observed. Our experiments showed that the ED patterns on different nanowires and different positions of an individual nanowire were essentially the same, implying that the chitosan nanowires are single crystalline in nature. The X-ray diffraction (XRD) pattern provides further confirmation of the crystallinity of the chitosan nanowires (not shown here). The characteristic reflection at $2\theta = 21.6^\circ$ corresponds to the orthorhombic crystal structure of chitosan (JCPDS no. 39-1894). It is first reported here that single-crystal chitosan nanowires can be prepared by a nonaqueous electrochemical approach.

In order to examine further the growth of chitosan nanowires by the electrochemical preparation reported here, the evolution of nanowires with deposition time was studied. Figure 2 shows SEM images of chitosan electrochemically deposited for 30 s, 3 min, or 6 min. After 30 s of deposition, nanoparticles (NPs) with an average size of ca. 75 nm can be observed (Fig. 2a). Some NPs are as small as ca. 10 nm in diameter, indicating that chitosan NPs as nuclei or seeds for subsequent growth were formed primarily on the substrate. We propose that these NPs possess high crystallinity and their initial embryos were already formed by self-assembly in solution before electrodeposition. It is well known that chitosan is soluble in acidic aqueous solution. Here, in our case, chitosan was firstly introduced into acidified PC solution (pH adjusted to ca. 4.5). As the solubility of chitosan in acidified PC is much less than in acidic aqueous solution, and the as-received chitosan powder does show some crystallinity already (see Fig. S1 in the Supporting Information), chitosan is expected to exist in a crystalline embryonic form and to suspend in the acidified organic system with the help of mild

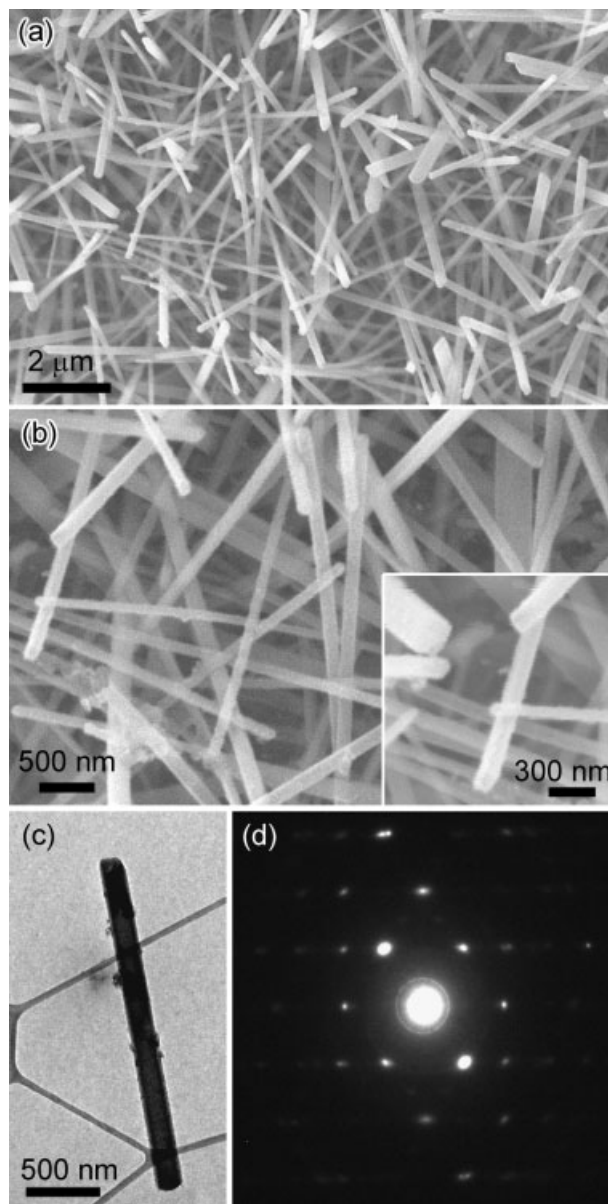


Figure 1. a,b) SEM images of chitosan nanowires deposited at $E = -3$ V vs. Ag/AgCl for 10 min. Inset in (b): Enlarged SEM image showing the rectangular cross section of the chitosan nanowires. c) TEM image of a typical chitosan nanowire. d) Electron diffraction pattern of the chitosan nanowire in (c).

ultrasonication, instead of being completely dissolved. These chitosan NPs should be slightly positively charged due to the acidification of the amine groups; that is, they are attracted towards the cathode. Meanwhile, H^+ ions around the cathode are effectively reduced, resulting in a gradual increase of pH near the cathode surface. Since the solubility of chitosan is pH-dependent,^[11] chitosan NPs can thus be first condensed onto the cathode surface under a uniform electric field. Although the crystallinity of these NPs cannot be directly confirmed because the NP coating is too thin for XRD measurement and they cannot be scrapped off the substrate

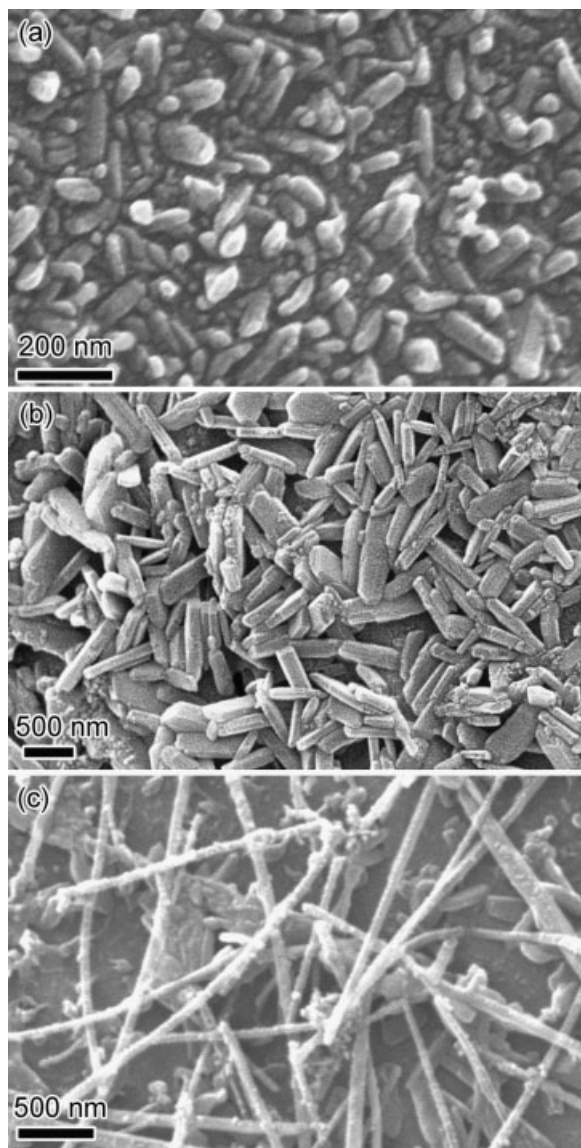


Figure 2. SEM images of chitosan electrochemical deposited at $E = -3$ V vs. Ag/AgCl for a) 30 s, b) 3 min, and c) 6 min with 5 mM LiClO₄ in PC solution.

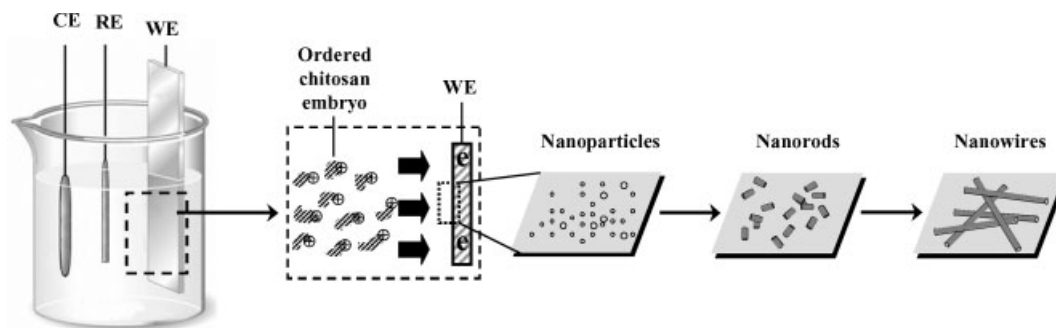
without any damage for TEM analysis, we have performed a special test to prove our proposed idea. In this special trial, we applied high-power ultrasonication (650 W for 120 min) to one chitosan solution before electrodeposition, so as to completely avoid formation of any self-assembled chitosan embryos. The treated solution was then used for electrodeposition under the same conditions as the others. It was found that no nanostructured chitosan could be prepared using this chitosan solution specifically treated with high-power ultrasonication. In the meantime, rectangular embryos have been actually observed by TEM analysis of samples collected from normal chitosan solution (without high-power ultrasonication) before electrodeposition (see Fig. S1 in the Supporting Information). As such, we propose that the chitosan embryos formed from

the solution without being treated with high power ultrasonication at the initial stage should be highly crystalline, and these highly crystalline embryos are pivotal to the subsequent growth of nanostructures in our electrochemical synthesis by serving as crystalline seeds. In fact, because of the limited solubility of chitosan in nonaqueous solvent (PC in this case), formation of highly crystalline embryos by self-assembly within the solvent is allowed. After this “incubation” process, highly crystalline chitosan NPs can be first deposited onto the cathodic substrate, paving the way for further growth of various crystalline chitosan nanostructures.

After deposition of NPs, when the deposition time was prolonged to 3 min, 1D nanorods of chitosan with an average diameter and length of 75 nm and 0.5 μ m, respectively, were observed. When the deposition time was extended to 6 min, the aspect ratio increased, and nanowires were formed. Their lengths were up to ca. 1 μ m, but their diameters did not change obviously (Fig. 2c). Finally, long nanowires were synthesized after 10 min of electrodeposition (Fig. 1a). As such, it is reasonably proposed that positively charged chitosan embryos in an acidic organic medium can be attracted and deposited on the substrate surface, forming crystalline NPs under the applied electric field. Then the growth of these NPs proceeds to nanorods, and finally to uniform single-crystalline nanowires (Scheme 1).

Although successful synthesis of chitosan nanostructures by such an electrochemical approach was demonstrated, further investigations have been made to examine the control of nanomorphology by changing the experimental conditions. Here, the effects of the applied potential (E) and the electric current (I), which specifically indicates the deposition rate, are the prime subjects for study. Figure 3 shows SEM images of chitosan nanostructures synthesized at potentials of -1 and -5 V versus Ag/AgCl. It is obvious that upon increasing the magnitude of E , the morphology of chitosan changed from nanoflakes (Fig. 3a) to nanowires (Fig. 1a), and then to mixed nanowires, nanobelts, and finally thick nanorods (Fig. 3b). In addition, in a separate experiment, when chitosan solution was simply drop-cast onto a substrate (which was equivalent to a deposition at $E = 0$ V), only featureless chitosan particles formed, without any specific nanoscale morphology. The results show that the application of an electric potential E is essential for the formation of chitosan nanostructures. The ultimate morphology is, in fact, E -dependent. The detailed mechanism accounting for the E -dependence of chitosan nanoscale morphology remains unclear at the moment. However, this E -dependence implies that the formation of chitosan nanostructures requires additional energy. We propose that the additional energy allows more possible configurations of molecular packing, which should be originally restricted to a layered molecular structure bounded by the intra- and intermolecular hydrogen bonds as described by Okuyama et al.^[12] In fact, at low E ($E = -1$ V), planar nanoflakes were observed.

Electric current I is another crucial factor in general electrochemical synthesis. It directly reflects the deposition



Scheme 1. Illustration of the growth of chitosan nanowires (CE, RE, and WE denote the counter, reference, and working electrodes, respectively).

rate of synthesis. In our experiments, I was adjusted by varying the concentration of LiClO_4 that serves as a supporting electrolyte. Increased concentration of the LiClO_4 results in increased I . Figure 4 shows SEM images of chitosan nanostructures synthesized at different concentrations of LiClO_4 , and thus different I . In addition to nanowires, other morphologies, including nanobelts and tapered nanoflakes, can be tuned by controlling the concentration of the supporting electrolyte. With an increase of the deposition rate, the width of nanobelts and nanoflakes becomes large compared with that of the nanowires (Fig. 1). Some nanobelts or nanoflakes can have widths up to ca. 600 nm or even larger (Fig. 4).

Interestingly, they evolved into nanotubes (ca. 250 nm in diameter) when the deposition time was prolonged to 30 min (Fig. 4d). The formation of nanotubes may arise from the scrolling of nanobelts and nanoflakes. By carefully examining the SEM images, scrolling behavior into nanotubes can indeed be observed (see bottom-right inset in Fig. 4d). Similar behavior has been reported for the formation of inorganic nanotubes.^[13] We propose that due to the limited solubility of chitosan in acidified PC, the ever-growing chitosan nanobelts or nanoflakes would tend to scroll up in order to minimize the surface energy. As a result, nanotubes are formed after prolonged electrodeposition. More experiments are in progress to study the detailed formation mechanism of these nanotubes.

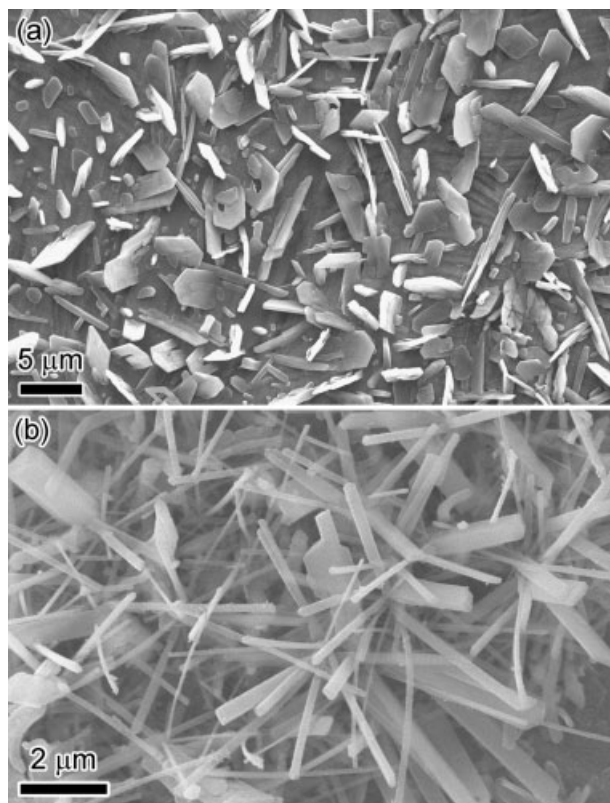


Figure 3. SEM images of chitosan electrochemically deposited at a) -1 V and b) -5 V vs. Ag/AgCl .

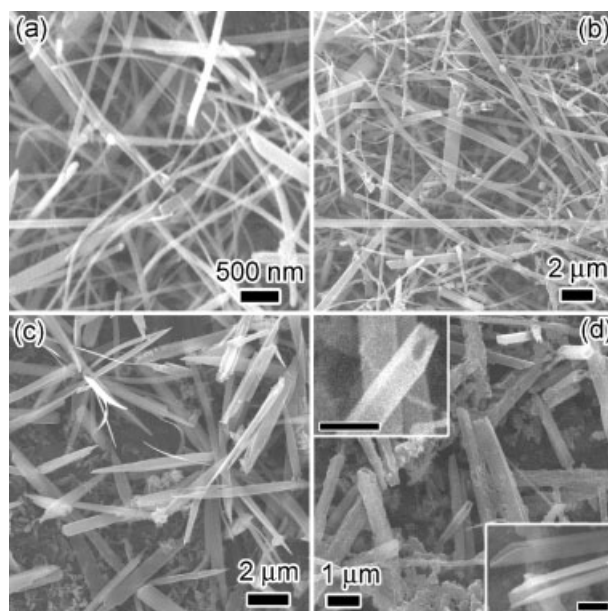


Figure 4. SEM images of chitosan electrochemically deposited at -3 V for 10 min with a concentration of LiClO_4 of a) 13.8 mM, b) 27.5 mM, and c) 55 mM, which correspond to currents of 1.9 mA, 3.5 mA, and 4.5 mA, respectively. d) SEM image of chitosan, as in (c) but with deposition time increased to 30 min. Insets: Enlarged SEM images of typical nanotubes. Scale bars in the insets: 500 nm.

In conclusion, we have demonstrated a simple, convenient, nonaqueous electrochemical approach to fabricating various single-crystal chitosan nanostructures. This approach does not require a template, catalysis, or surfactant, and therefore it is ideal for exploring large-scale industrial production of chitosan nanomaterials. The chitosan nanostructures as grown by adjusting the deposition time, electrochemical potential, and the electric current, provide a variety of nanomorphologies for further applications and studies, for example, cell adhesion, in vitro cell proliferation, tissue-compatible scaffolds, and nanostructure-based sensors. Considering the proven versatility and biocompatibility of chitosan, chitosan nanowires may find profound applications in nanodevices, and in the medical and pharmaceutical fields.

Experimental

Chitosan with an 85% degree of deacetylation was obtained from Sigma. PC (99.7%, Sigma) and lithium perchlorate (LiClO_4 , BDH Chemicals Ltd., Poole, UK) were used as received. In a typical experiment, 8.5 mg chitosan was dispersed into 45 mL acidified PC solution under mild ultrasonication for 2 h. The solution was at ca. pH 4.5, adjusted by adding drops of aqueous H_2SO_4 . Stainless steel foils ($0.5\text{ cm} \times 2.5\text{ cm} \times 0.075\text{ cm}$, AISI 304), were purchased from Goodfellow Cambridge Ltd. and were used as a substrate for deposition. Electrochemical experiments were performed on a CHI 660A computerized electrochemical workstation (CHI, USA) by the potentiostatic method. A three-electrode system was used, including a stainless steel foil as the working electrode ($0.5\text{ cm} \times 2.5\text{ cm}$), an anhydrous reference electrode (Ag/AgCl), and a platinum coil as the counter electrode. The general morphology of the products was characterized by SEM (LEO, 1450VP). Electron diffraction patterns were obtained by TEM (Philips CM 120, 120 kV). XRD patterns were collected with a Bruker D8 Advance diffractometer with high-intensity $\text{Cu K}\alpha_1$ irradiation ($\lambda = 1.5406\text{ \AA}$).

Received: July 27, 2007

Revised: November 26, 2007

Published online: May 5, 2008

- [1] See, e.g., a) E. Dujardin, S. Mann, *Adv. Mater.* **2002**, *14*, 775. b) N. A. Peppas, J. Z. Hilt, A. Khademhosseini, R. Langer, *Adv. Mater.* **2006**, *18*, 1345.
- [2] See, e.g., a) C. Y. Zhang, H. C. Yeh, M. T. Kuroki, T. H. Wang, *Nat. Mater.* **2005**, *4*, 826. b) M.-C. Daniel, D. Astruc, *Chem. Rev.* **2004**, *104*, 293. c) H. Li, J. Huang, J. Lv, H. An, X. Zhang, Z. Zhang, C. Fan, H. Hu, *Angew. Chem. Int. Ed.* **2005**, *44*, 5100.
- [3] a) M. Reches, E. Gazit, *Nat. Nanotechnol.* **2006**, *1*, 195. b) S. Vauthey, S. Santoso, H. Y. Gong, N. Watson, S. Zhang, *Proc. Natl. Acad. Sci.* **2002**, *99*, 5355. c) J. D. Hartgerink, E. Beniash, S. I. Stupp, *Science* **2001**, *294*, 1684.
- [4] a) S. B. Park, J. O. You, H. Y. Park, S. J. Haam, W. S. Kim, *Biomaterials* **2001**, *22*, 323. b) Y. P. Mehrdad, R. Jaime, Q. Raul, *Macromol. Chem. Phys.* **2000**, *201*, 923.
- [5] a) T. Suzuki, T. Matsumoto, Y. Hagino, in *Science and Technology of Polymers and Advanced Materials* (Eds: P. N. Prasad, J. E. Mark, S. H. Kandil, Z. H. Kafafi) Plenum, New York **1998**, pp. 567–571. b) *Material Science of Chitin and Chitosan* (Eds: T. Urugami, S. Tokura) Kodansha Springer, Tokyo **2006**, p. 4.
- [6] a) P. J. VandeVord, H. W. T. Matthew, S. P. DeSilva, L. Mayton, B. Wu, P. H. Wooley, *J. Biomed. Mater. Res.* **2002**, *59*, 585. b) H. Onishi, Y. Machida, *Biomaterials* **1999**, *20*, 175. c) F. E. Black, M. Hartshorne, M. C. Davies, C. J. Roberts, S. J. B. Tendler, P. M. Williams, K. M. Shakesheff, S. M. Cannizzaro, I. Kim, R. Langer, *Langmuir* **1999**, *15*, 3157.
- [7] a) X. L. Luo, J. J. Xu, J. L. Wang, H. Y. Chen, *Chem. Commun.* **2005**, 2169. b) R. A. Langer, *Chem. Res.* **2000**, *33*, 94. c) S. Ishaug-Riley, L. L. E. Okun, G. Prado, M. A. Applegate, A. Ratcliffe, *Biomaterials* **1999**, *20*, 2245.
- [8] a) R. Langer, D. A. Tirrell, *Nature* **2004**, *428*, 487. b) M. N. Kumar, R. A. Muzzarelli, C. Muzzarelli, H. Sashiwa, A. J. Domb, *Chem. Rev.* **2004**, *104*, 6017.
- [9] a) M. N. V. R. Kumar, *React. Funct. Polym.* **2000**, *46*, 1. b) Y. J. Park, Y. M. Lee, S. N. Park, S. Y. Sheen, C. P. Chung, S. J. Lee, *Biomaterials* **2000**, *21*, 153. c) A. Gutowska, B. Jeong, M. Jasionowski, *Anat. Res.* **2001**, *263*, 342. d) H. Tamura, Y. Tsuruta, K. Itoyama, W. Worakitkanchanakul, R. Rujiravanit, S. Tokura, *Carbohydr. Polym.* **2004**, *56*, 205. e) N. Iwasaki, S. T. Yamane, T. Majima, Y. Kasahara, A. Minami, K. Harada, S. Nonaka, N. Maekawa, H. Tamura, S. Tokura, M. Shiono, K. Monde, S. I. Nishimura, *Biomacromolecules* **2004**, *5*, 828. f) T. Funakoshi, T. Majima, N. Iwasaki, S. Yamane, T. Masuko, A. Minami, K. Harada, H. Tamura, S. Tokura, S. I. Nishimura, *J. Biomed. Mater. Res.* **2005**, *74A*, 338.
- [10] a) N. Bhattarai, D. Edmondson, O. Veis, F. A. Matsen, M. Q. Zhang, *Biomaterials* **2005**, *26*, 6176. b) K. Ohkawa, K.-I. Minato, G. Kumagai, S. Hayashi, H. Yamamoto, *Biomacromolecules* **2006**, *7*, 3291.
- [11] R. Fernandes, L. Q. Wu, T. Chen, H. Yi, G. W. Rubloff, R. Ghodssi, W. E. Bentley, G. F. Payne, *Langmuir* **2003**, *19*, 4058.
- [12] K. Okuyama, K. Noguchi, T. Miyazawa, T. Yui, K. Ogawa, *Macromolecules* **1997**, *30*, 5849.
- [13] a) Z. V. Saponjic, N. M. Dimitrijevic, D. M. Tiede, A. J. Goshe, X. B. Zuo, L. X. Chen, A. S. Barnard, P. Zapol, L. Curtiss, T. Rajh, *Adv. Mater.* **2005**, *17*, 965. b) W. X. Zhang, X. G. Wen, S. H. Yang, Y. Berta, Z. L. Wang, *Adv. Mater.* **2003**, *15*, 822.